The Effect of Preheating on the Quality of Spot Welding Between Dissimilar Mild Steel and Stainless Steel 304

Kristiana Pasau [1,2], Nasaruddin Salam [1], Ahmad Yusran Aminy [1], and Azwar Hayat [1,*]

[1] Department of Mechanical Engineering, Faculty of Engineering, Hasanuddin University, Makassar, Indonesia
[2] Department of Mechanical Engineering, Faculty of Engineering, Universitas Kristen Paulus Makassar, Makassar, Indonesia
Email: kristianapasau@gmail.com (K.P.); nassalam.unhas@yahoo.co.id (N.S.); ahmadyusran179@gmail.com (A.Y.A.); azwar.hayat@unhas.ac.id (A.H.)
*Corresponding author

***Abstract*—Resistance Spot Welding (RSW) is widely used in automotive and manufacturing industries for joining metallic sheets; however, welding dissimilar metals such as mild steel and stainless steel remains challenging due to their differing thermal and metallurgical properties. This study investigates the influence of preheating the stainless steel component at varying temperatures (100 °C, 120 °C, 150 °C, and 180 °C) on the mechanical and microstructural characteristics of dissimilar RSW joints with mild steel. Tensile testing, hardness profiling, and Scanning Electron Microscopy/Energy Dispersive Spectroscopy (SEM/EDS) analyses were conducted to evaluate joint performance. The results revealed that preheating significantly affects residual stress distribution, ductility, and joint homogeneity. Without preheating, joints exhibited high tensile strength (127.46 MPa) but low ductility due to rapid cooling and martensitic formation. Optimal conditions were achieved at 180 °C preheat, yielding the highest tensile strength (156.32 MPa), improved ductility (strain = 1.80% Gauge Length), and the lowest standard deviation (6.95 MPa), indicating enhanced process stability. Hardness analysis confirmed a balanced gradient across the weld, heat-affected zone, and base metal, while SEM observations identified reduced microcracks and improved microstructural uniformity at higher preheat levels. Overall, a preheat temperature of 180 °C effectively minimizes thermal gradients and residual stresses, improving weld integrity and consistency. These findings provide practical insights for optimizing preheating parameters in industrial RSW applications, particularly in the fabrication of automotive body structures and other dissimilar steel assemblies.**

***Keywords*—preheat, dissimilar material, resistance spot welding**

I. Introduction

Welding is a fundamental manufacturing process extensively utilized across various industries due to its capability to fabricate complex geometric joints in diverse metals and thicknesses [1]. Among these techniques, Resistance Spot Welding (RSW) serves as a primary assembly method for automotive, aerospace, and marine body-in-white structures, renowned for its simplicity, cost-effectiveness, high efficiency, and adaptability to automation [2–4]. However, joining dissimilar materials via RSW presents inherent challenges. Differences in critical thermophysical properties, such as melting point and electrical conductivity, lead to asymmetric heat generation and distribution at the weld interface, consequently compromising joint integrity [5, 6]. Improper control of welding parameters often results in defects including incomplete penetration, cracking porosity, and excessive spatter [7, 8].

Existing research on RSW of dissimilar metals has predominantly focused on two strategies: optimizing process parameters and modifying the weld interface. For instance, in mild steel–stainless steel combinations, factors such as nugget size, welding current, and sheet thickness are identified as primary determinants of joint strength [9, 10]. For metallurgically incompatible pairs like aluminum–steel or titanium–stainless steel, the incorporation of composite electrodes or copper interlayers has been demonstrated to suppress the formation of brittle intermetallic compounds, thereby enhancing mechanical performance [11, 12]. Similarly, in mild steel–galvanized steel welds, welding current is the dominant parameter, while force and time require careful optimization based on material characteristics [13]. Furthermore, failure mechanisms in mild steel–stainless steel joints, often associated with tensile stress concentration and thinning in the Heat-Affected Zone (HAZ), can be mitigated through surface roughening techniques prior to welding [14, 15].

Concurrently, preheating has been established as a robust thermal management strategy in various other welding processes to control heat transfer, minimize residual stresses, and improve joint quality. In solid-state welding, Induction-Assisted Friction Stir Welding

Manuscript received September 18, 2025; revised September 29, 2025; accepted October 20, 2025; published January 23, 2026.

(I-FSW) of superalloys like Inconel 718 to SS316L demonstrates that preheating improves material plasticity, refines grain structure, reduces axial forces, and achieves joint strengths approaching those of the base metals [16–18]. In fusion-based processes, preheating in laser welding of AISI 420 martensitic stainless steel and in spot welding of aluminum alloys has proven effective in minimizing solidification cracking and stabilizing weld nugget formation by reducing thermal gradients [19–21]. Within arc welding techniques such as Gas Metal Arc Welding (GMAW) and Gas Tungsten Arc Welding (GTAW), preheating is recognized for optimizing tensile strength and toughness in dissimilar joints, such as those between aluminum and stainless steel or medium-mild steels, while simultaneously reducing porosity [22, 23]. Systematic studies on GMAW of AISI 304 and ASTM A36 steel have confirmed that moderate preheating yields an optimal balance of strength and toughness [24], with optimization models identifying it as a critical parameter second only to welding speed [25]. Investigations into Shielded Metal Arc Welding (SMAW) of various steels further corroborate that elevated preheating temperatures reduce cooling rates, suppress hydrogen-induced cracking, and enhance fracture toughness through microstructural refinement [26, 27]. Beyond ferrous alloys, heat-assisted welding of BeAl systems has been shown to improve plastic flow and hardness despite limitations in tensile strength [28].

Collectively, these studies highlight the significant role of preheating in enhancing weldability across diverse materials and processes. However, a critical research gap remains regarding its systematic application in RSW of dissimilar steels. Existing work has largely concentrated on fusion and solid-state methods, leaving the influence of preheating on the mechanical properties, microstructural evolution, and failure mechanisms of RSW joints—particularly between mild steel and AISI 304 stainless steel—insufficiently understood.

This research explores how variations in preheat temperature applied to mild steel and stainless steel AISI 304 before welding can affect the mechanical properties of weld joints in the resistance spot welding process. This offers new insights into preheat temperatures to improve weld joint quality. Then, the mechanical properties of resistance spot welding joints between mild steel that did not receive special treatment and AISI 304 stainless steel preheated at various temperatures were compared. This will help identify how preheating stainless steel can improve joint quality, even when mild steel is not preheated. In addition, systematic data that combines tensile testing, hardness testing, and microstructural analysis using Scanning Electron Microscopy/Energy Dispersive Spectroscopy (SEM/EDS) is not yet available. Thus, this study presents a novelty by comprehensively investigating the effect of preheating temperature on RSW of mild steel–AISI 304 Stainless steel, so that it can provide new understanding as well as a basis for optimizing preheating parameters to improve the quality of joints in dissimilar steel materials.

II. Materials and Methods

The materials used in this study are mild steel and stainless steel AISI 304 plates with specimen dimensions of 100×25×1 mm, as shown in Fig. 1. The results of welding mild steel and stainless steel preheated are shown in Fig. 2, while the results of welding mild steel without treatment and stainless steel preheated are shown in Fig. 3.

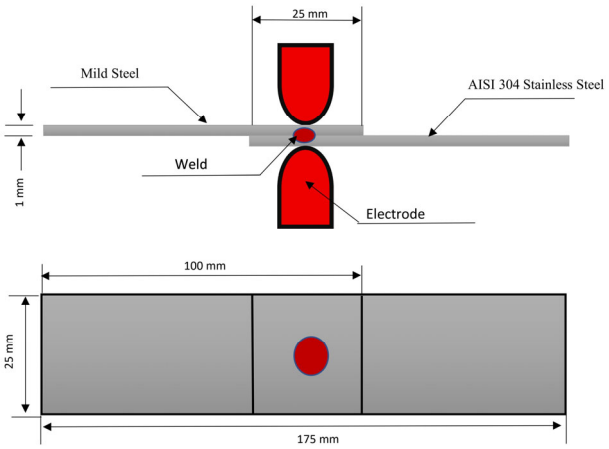

Fig. 1. Schematic diagram of the test object used in the research.

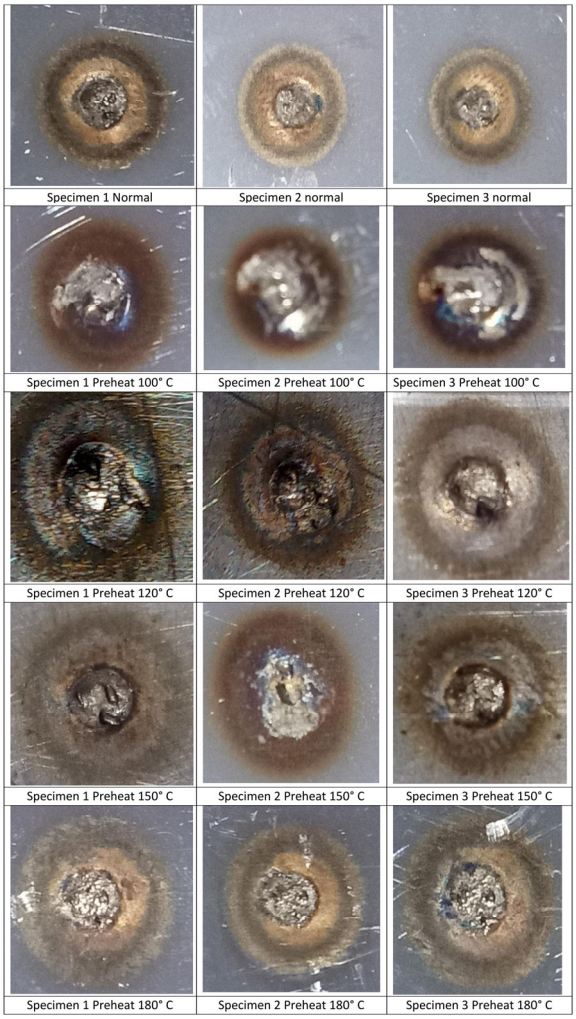

Fig. 2. Specimen of mild steel and stainless steel welding results in preheat.

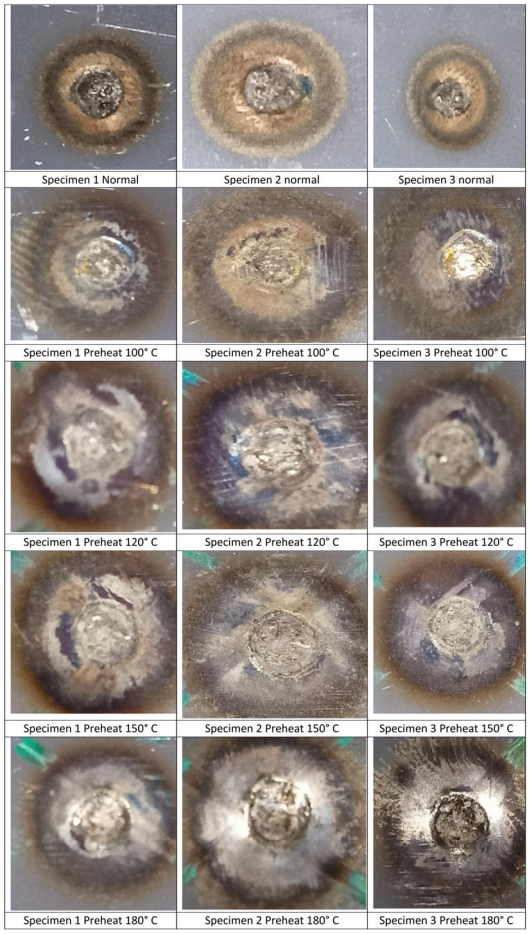

Fig. 3. Specimen of mild steel welding without treatment and stainless steel in preheat.

The welding process employs a hydraulic air-pressure electrode system equipped with a pressure adjustment mechanism, where the welding current is controlled through an analog system and the welding time is regulated digitally, as illustrated in Fig. 4. The spot welding operation utilizes the following parameters: a welding current of 6000 A, a welding duration of 6 seconds, and an electrode pressure of 40 psi, using a DN-16 type spot weld electrode. These settings provide optimal joint quality by ensuring precise control over current, time, and electrode pressure throughout the welding process.

Fig. 4. Resistance spot welding.

Preheat treatment is the initial heating of metal materials before welding, aimed at reducing residual stress, improving weld quality, controlling heat transfer, and preventing crack formation. Preheated was done in Nabertherm muffle furnace, as illustrated in Fig. 5. This study employs two distinct treatments.

(1) Preheating treatment is applied to mild and stainless steel AISI 304 plates.
(2) Treatment of mild steel plates without special treatment and stainless steel 304 plates with preheating treatment.

The preheat temperature range (100 °C, 120 °C, 150 °C, and 180 °C) was chosen to ensure adequate reduction of thermal gradients while avoiding excessive softening or structural alteration of the base metals [29, 30]. Preheating was selectively applied to stainless steel plates because of their lower thermal conductivity and higher coefficient of thermal expansion, which make them more susceptible to thermal cracking compared to mild steel. For each preheat temperature condition, three specimens were prepared (n = 3). The mean and standard deviation of tensile strength and hardness results were calculated to evaluate the reproducibility of the experiments.

Fig. 5. Furnace used for specimen preheating.

Uniaxial tensile testing was carried out pursuant to the guidelines of ASTM E8M. A Universal Testing Machine (UTM) was employed, wherein specimens were mounted in the machine's grips. Precise axial alignment between the specimen and the force axis was ensured to mitigate the introduction of bending stresses. A tensile speed of 3 mm/min was applied, as stipulated by the standard for the evaluation of sheet-type materials [31].

Rockwell hardness testing was performed following the ASTM E18 standard, utilizing a 120° diamond cone indenter and a 150 kgf applied load. Each specimen was assessed with three impressions at designated locations: the base metal, the HAZ, and the weld area, to obtain a representative hardness distribution [32, 33].

The present study aims to provide a microstructural and compositional analysis of RSW joints fabricated from dissimilar materials: mild steel and AISI 304 stainless steel. The core of the research involves utilizing SEM/EDS techniques, with a particular focus on elemental mapping. This approach is deployed to systematically investigate how variations in preheat temperature affect the interdiffusion of key constituent elements—Iron (Fe),

Chromium (Cr), and Nickel (Ni)—at the weld interface. The analysis of these elemental distribution profiles is critical for understanding their subsequent impact on the formation of intermetallic phases and defect generation, which ultimately govern joint quality. The findings are anticipated to yield critical insights into the efficacy of preheat treatment as a process parameter for enhancing the mechanical properties and long-term durability of dissimilar steel RSW joints [34, 35].

III. Result and Discussion

A. The Process of Plating Mild Steel and Stainless Steel 304 Involves Preheating the Raw Materials

Tensile testing is conducted to assess the strength of the spot welding joint between mild steel and stainless steel materials. In this test, various treatments were applied to the material, namely without preheat treatment, as well as preheat at temperatures of 100 °C, 120 °C, 150 °C, and 180 °C. Each treatment involves testing three specimens to obtain accurate and representative data. The tensile test data for treated mild steel and stainless steel plates with preheating treatment is shown in Table I.

As delineated in Fig. 6 and Table I, the tensile test results for the resistance spot welds between mild steel and stainless steel elucidate a significant influence of preheating on the joint's tensile strength, elongation, and performance consistency. In the absence of preheating (normal condition), the joints exhibited a high average tensile strength of 127.46 MPa (SD = 12.04 MPa), coupled with an average strain of −0.69% Gauge Length (GL) (SD = 0.17% GL). This elevated strength is attributed to the rapid cooling rate post-welding, which promotes the formation of hard, brittle microstructures, such as martensite, particularly on the mild steel side. Despite the high strength, this condition results in significant residual stresses due to the disparate thermal properties of the two materials, thereby increasing the susceptibility to micro-cracking and compromising long-term fatigue resistance.

TABLE I. Tensile Test Data for Mild Steel and Stainless Steel Plates with Preheating Treatment

Preheat	Variation Preheat	Specimen			Average	Standard Deviation
		1	2	3		
Without	Stress (MPa)	114.06	130.96	137.36	127.46	12.04
	Strain (% GL)	−0.88	−0.64	−0.56	−0.69	0.17
100 °C	Stress (MPa)	90.31	110.80	91.93	97.68	11.39
	Strain (% GL)	−0.88	0.68	−1.06	−0.42	0.96
120 °C	Stress (MPa)	155.14	70.95	110.66	112.25	42.12
	Strain (% GL)	−0.80	−3.80	−1.62	−2.07	1.55
150 °C	Stress (MPa)	94.18	130.39	127.80	117.46	20.20
	Strain (% GL)	−0.64	1.75	−1.06	0.02	1.52
180 °C	Stress (MPa)	117.68	118.31	129.31	121.77	6.54
	Strain (% GL)	−0.77	−0.85	−0.35	−0.66	0.27

The application of preheating demonstrated a trade-off, generally reducing tensile strength while enhancing the stability of the weld properties. At a preheat temperature of 100 °C, the tensile strength decreased to an average of 97.68 MPa (SD = 11.39 MPa) with a strain of −0.42% GL (SD = 0.96% GL), indicating its insufficiency in effectively mitigating the thermal gradient. A preheat of 120 °C yielded an increased average strength of 112.25 MPa; however, the high standard deviation of 42.12 MPa suggests inconsistent heat distribution. A more balanced condition was observed at 150 °C, with a tensile strength of 117.46 MPa (SD = 20.20 MPa) and a marked improvement in ductility, evidenced by a strain value of 0.02% GL (SD = 1.52% GL).

The most stable and reproducible results were achieved at a preheat temperature of 180 °C. This condition produced a tensile strength of 121.77 MPa with the lowest standard deviation of 6.54 MPa and a strain of −0.66% GL (SD = 0.27% GL), signifying superior uniformity in weld quality. The marginal decrease in strength compared to the non-preheated condition does not denote joint weakness. Instead, it reflects the beneficial role of preheating in reducing residual stress and slowing the cooling rate, thereby suppressing the formation of brittle martensite.

In conclusion, the primary benefit of preheating is not to maximize tensile strength, but to enhance joint integrity by alleviating internal stresses, homogenizing the microstructure, improving ductility, and consequently extending the service life of the weld. The temperature range of 150–180 °C is identified as the optimal window, effectively balancing strength, stability, and long-term durability.

Material hardness analysis in welding mild steel and stainless steel with preheat treatment aims to understand the effect of preheating on the hardness characteristics in the weld area, HAZ, and base metal.

The hardness measurements across the weld zone, HAZ, and base metal, as summarized in Table II, provide critical insight into the microstructural evolution induced by preheating in dissimilar steel joints. The data clearly demonstrate that the preheat treatment significantly influences the hardness profile of the weldment.

In the weld zone, the average hardness decreased from 108.7 HRC at 100 °C preheat to 106.4 HRC at 180 °C. This trend can be attributed to a slower cooling rate facilitated by preheating, which mitigates the formation of excessive martensite and promotes a more tempered, ductile microstructure. Although the highest average hardness was recorded at 100 °C preheat (108.7 HRC), the lower standard deviation observed at 180 °C suggests a more consistent and homogeneous microstructure, aligning with the improved joint stability noted in the tensile tests.

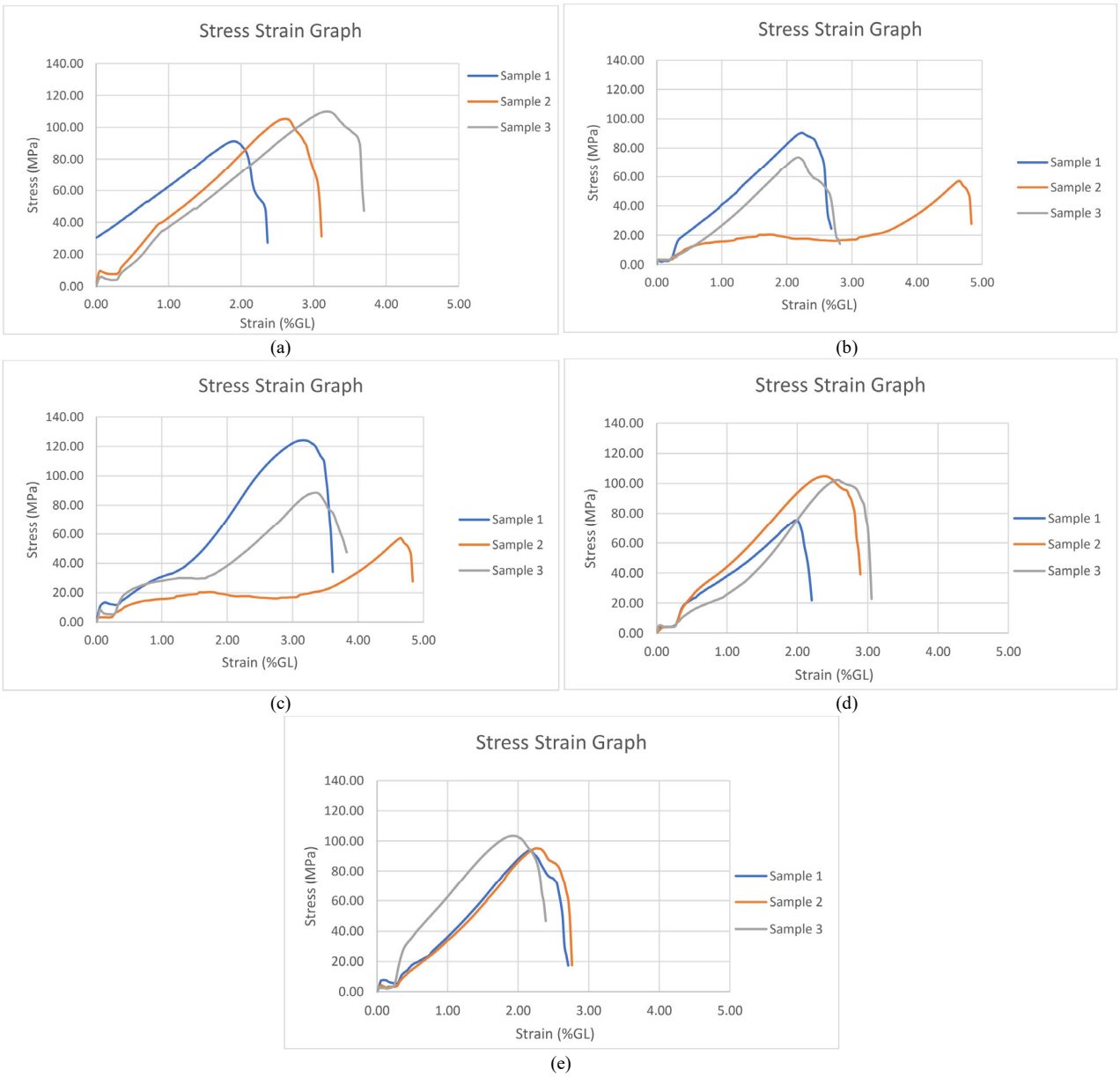

Fig. 6. Stress–strain graphs of welded specimens at different preheat temperatures. (a) Without preheat; (b) Preheat 100 °C; (c) Preheat 120 °C; (d) Preheat 150 °C; (e) Preheat 180 °C.

TABLE II. TEST DATA FOR THE HARDNESS OF MILD STEEL AND STAINLESS STEEL WELDING MATERIALS WITH PREHEAT TREATMENT IS AVAILABLE

Preheat	Weld area (HRC)	Average	HAZ (HRC)	Average	Base Metal (HRC)	Average
Without	100.3	102.3	88.1	83.3	98.1	98.4
	102.1		86.5		96.9	
	104.4		75.3		100.1	
100 °C	109.0	108.7	93.6	95.1	93.9	94.1
	112.7		95.3		93.2	
	104.5		96.4		95.1	
120 °C	105.9	106.1	96.7	96.7	98.1	103.9
	107.9		99.1		112.2	
	104.6		94.3		101.3	
150 °C	103.2	108.5	98.9	93.2	96.6	94.7
	113.2		92.0		94.1	
	109.0		88.6		93.4	
180°C	103.5	106.4	84.1	88.6	99.1	99.5
	111.1		90.0		104.0	
	104.6		91.8		95.3	

The HAZ exhibited the most pronounced sensitivity to preheat temperature. The average hardness peaked at 96.7 HRC with a 120 °C preheat, indicating a critical thermal condition that potentially maximizes solid solution strengthening or secondary phase precipitation. However, the subsequent decline in hardness to 88.6 HRC at 180 °C reflects the dominance of tempering effects and recovery processes, which soften the microstructure. This reduction in HAZ hardness is beneficial for mitigating crack susceptibility and improving the overall toughness of the joint.

Conversely, the base metal hardness remained relatively stable across all conditions, with values fluctuating within a narrow range (94.1 to 103.9 HRC). This consistency confirms that the thermal cycles from welding and preheating had a negligible effect on the bulk properties of the parent materials, as expected.

The inverse correlation observed between preheat temperature and weld zone hardness, coupled with the non-monotonic response of the HAZ, underscores the complex thermo-metallurgical interactions in dissimilar welding. The optimal preheat condition of 150–180 °C, identified from tensile testing, is further supported by this hardness analysis. Within this range, the joint achieves a favorable balance: a moderately hard yet ductile weld metal, a sufficiently toughened HAZ, and minimal residual stress concentrations, thereby enhancing the structural integrity and service reliability of the weldment.

Fig. 7 presents the SEM analysis of the weld specimen fabricated without preheating. At 100× magnification, the micrograph reveals several microscopic discontinuities within the weld metal, indicative of sub-optimal fusion. Spherical voids, characteristic of gas porosity, are observable and are likely attributable to entrapped gases or surface oxidation during the welding process.

A more detailed examination at 500× magnification provides higher-resolution insight into these surface anomalies. The image clearly delineates various solidification defects, including micropores, incipient microcracks, and localized textural variations resulting from the thermal cycling of welding. The presence of fissures adjacent to the weld zone suggests the development of significant thermal stress or inherent fusion imperfections.

(a) (b) (c)

Fig. 7. SEM images of specimens without preheat at different magnifications. (a) 100× magnification; (b) 500× magnification; (c) 2000× magnification.

Further elucidated at 2000× magnification, pronounced cracking is evident along the weld surface. These crack formations are consistent with solidification cracking mechanisms, predominantly initiated by the substantial differential thermal expansion between the dissimilar materials (mild steel and stainless steel). Furthermore, the rapid cooling rate inherent to the non-preheated condition induces high residual stresses, which exacerbate crack propagation and compromise the structural integrity of the joint.

Energy Dispersive X-ray Spectroscopy (EDS) analysis in Fig. 8 of the resistance spot weld joint between mild steel and stainless steel reveals a complex elemental composition comprising primary constituents including Fe, Cr, Ni, Manganese (Mn), Carbon (C), and Oxygen (O). The spectral data demonstrates prominent Fe and C peaks, confirming the substantial metallurgical influence of the mild steel component within the fusion zone. Concurrently, the detectable presence of Cr and Ni signatures confirms the successful integration of stainless steel elements into the weld microstructure.

The heterogeneous distribution of these alloying elements across the joint interface presents potential implications for joint integrity. Of particular significance is the elevated oxygen content identified in the spectrum, suggesting possible oxide formation during the welding process that may compromise the weld's structural continuity. Furthermore, the detection of trace elements including Chlorine (Cl), Aluminum (Al), and Silicon (Si) indicates potential exogenous contamination, possibly originating from surface conditions or auxiliary materials employed during fabrication.

The pronounced oxygen concentration at the weld interface signifies the development of surface oxides, which may adversely affect both the corrosion resistance and mechanical strength of the joint. This compositional analysis provides critical insight into the elemental intermixing behavior and identifies potential failure mechanisms in dissimilar metal welding, underscoring the importance of process control to minimize contamination and oxidation.

Fig. 9 presents the SEM analysis of the spot weld joint between mild steel and stainless steel, fabricated with a 150 °C preheat treatment, reveals several characteristic microstructural features at progressive magnification levels. At 100× magnification, the weld surface exhibits

discernible surface irregularities with distributed micro-porosity, potentially resulting from suboptimal material flow or oxide entrapment during the welding process.

When observed at 500× magnification, the interface region displays evident crack propagation, likely attributable to thermally induced stresses generated during the joining of these metallurgically dissimilar materials. The microstructural analysis at 2000× magnification further confirms the development of pronounced micro-cracking networks along the fusion zone, substantiating the presence of significant internal stresses arising from the differential thermal conductivity between the constituent materials.

Additionally, the persistent presence of porosity throughout the weld matrix suggests possible gas evolution during the thermal cycle, which collectively compromises the structural integrity of the joint. These observed defects underscore the challenging nature of dissimilar metal welding, even with the application of intermediate preheat treatments, highlighting the necessity for precise parameter optimization to achieve defect-minimized welds.

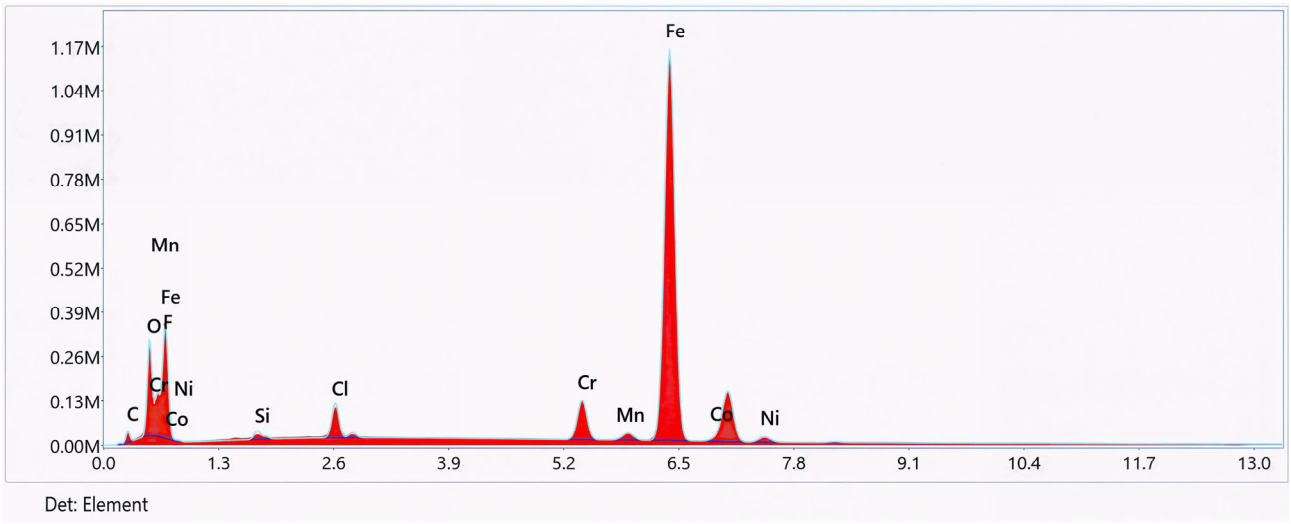

Fig. 8. Spectral results from Energy Dispersive X-ray Spectroscopy (EDS), specimen without preheat.

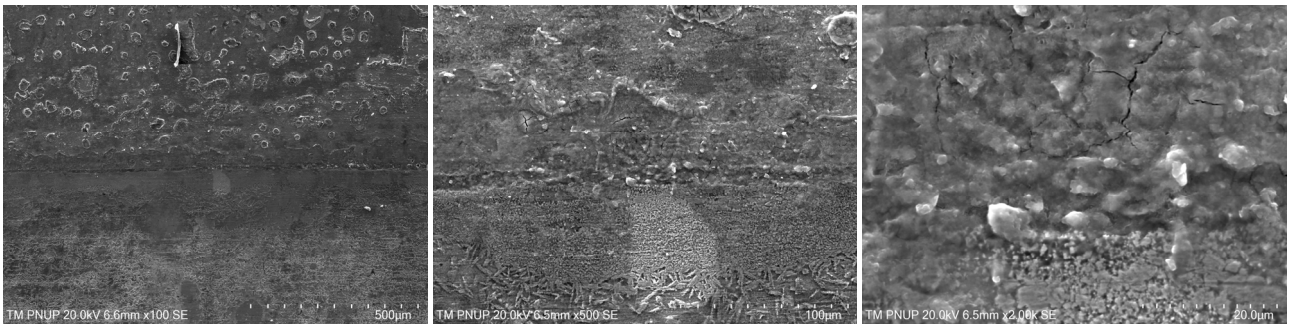

(a) (b) (c)

Fig. 9. SEM images of the specimen with 150 °C preheat at different magnifications. (a) 100× magnification; (b) 500× magnification; (c) 2000× magnification.

The Scanning Electron Microscopy/Energy Dispersive Spectroscopy (SEM/EDS) spectral analysis of the spot weld joint between mild steel and stainless steel shown in Fig 10, fabricated with a 150 °C preheat treatment, reveals a complex elemental composition characteristic of the dissimilar metal joining process. The spectrum exhibits a pronounced O peak at the initial energy range, suggestive of substantial surface oxidation enhanced by the elevated thermal input during the preheated welding cycle.

Critical alloying elements are identified at their characteristic energy levels: Mn appears at approximately 2.6 keV, functioning as a solid solution strengthener in both base materials. The dominant Fe peak at 6.3 keV confirms its primary constituent status in the weld matrix. A notable Cl signature detected at 2.5 keV potentially indicates surface contamination from processing environments or handling materials. The presence of Ni at 7.5 keV confirms the successful transfer of this crucial austenite-stabilizing element from the stainless steel component into the fusion zone, essential for maintaining corrosion resistance and mechanical strength in the composite joint.

This elemental profile demonstrates both the successful metallurgical integration of dissimilar materials and the concurrent challenges of oxidation and potential contamination inherent in the joining process.

Fig. 11 presents the SEM analysis of the dissimilar spot weld joint between mild steel and stainless steel, processed with a 180 °C preheat treatment, reveals distinctive surface characteristics across multiple magnification scales. At

100× magnification, the weld interface demonstrates considerable surface heterogeneity, featuring pronounced texture variations accompanied by micro-fissures and oxide layer formation. These morphological features are particularly evident in the mild steel region, where thermal stresses during the welding process have induced surface degradation and preferential oxidation.

Enhanced resolution at 500× magnification enables detailed observation of fine crack networks within the fusion zone, coexisting with particulate matter potentially derived from residual flux or external contaminants. The consistent presence of an oxide layer at this scale indicates potential compromise to the joint's interfacial integrity, which may negatively impact its long-term corrosion performance. At 2000× magnification, the analysis reveals comprehensive micro-crack systems and fine-scale particulate distribution, providing clear evidence of internal stress development attributable to the differential thermal expansion coefficients between the dissimilar materials. The oxide layer demonstrates significantly greater prevalence within the mild steel constituency, consistent with its inherent oxidative vulnerability.

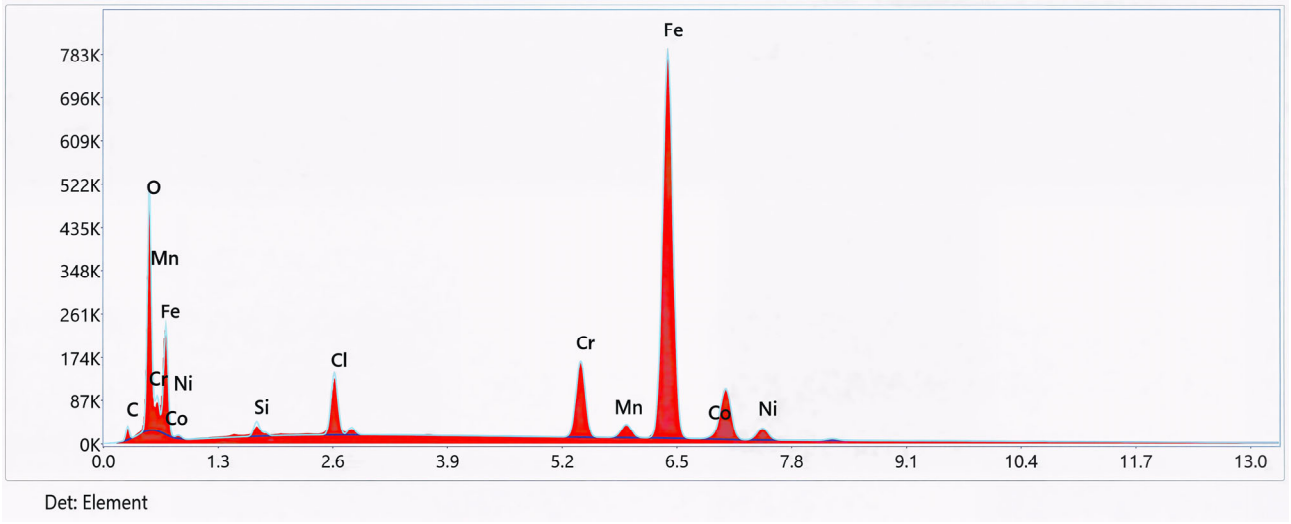

Fig. 10. Spectrum from EDS, specimen preheat 150 °C.

(a) (b) (c)

Fig. 11. SEM images of the specimen with 180 °C preheat at different magnifications. (a) 100× magnification; (b) 500× magnification; (c) 2000× magnification.

The comparative analysis conclusively demonstrates divergent material responses under identical thermal processing conditions, with stainless steel maintaining superior surface quality and oxidation resistance, while mild steel exhibits pronounced susceptibility to thermal degradation and oxidative attack, resulting in compromised surface morphology and potential long-term performance limitations.

Fig. 12 presents the EDS spectrum of the dissimilar spot weld joint between mild steel and stainless steel fabricated with a 180 °C preheat treatment, revealing significant elemental constituents and their implications for joint properties. The spectrum exhibits a prominent oxygen peak at approximately 0.5 keV, indicating substantial surface oxidation resulting from thermal exposure during the welding process. A significant carbon signature appears at 0.25 keV, confirming the substantial contribution from the mild steel component. The detection of chromium at 5.2 keV and nickel at 7.5 keV verifies the successful transfer of these crucial alloying elements from the stainless steel into the weld zone, essential for maintaining corrosion resistance and mechanical strength.

The dominant iron peak at 6.3 keV underscores its primary role as the base constituent of both materials, while manganese detected at 5.9 keV contributes to solid solution strengthening mechanisms. Notably, the presence of chlorine at 2.6 keV suggests potential contamination from processing environments or surface treatments, which may adversely affect joint integrity. This elemental profile demonstrates the complex metallurgical interaction

between the dissimilar materials and highlights both the successful alloy element transfer and the concurrent challenges of oxidation and potential contamination, providing crucial insights for optimizing welding parameters in dissimilar metal joining applications.

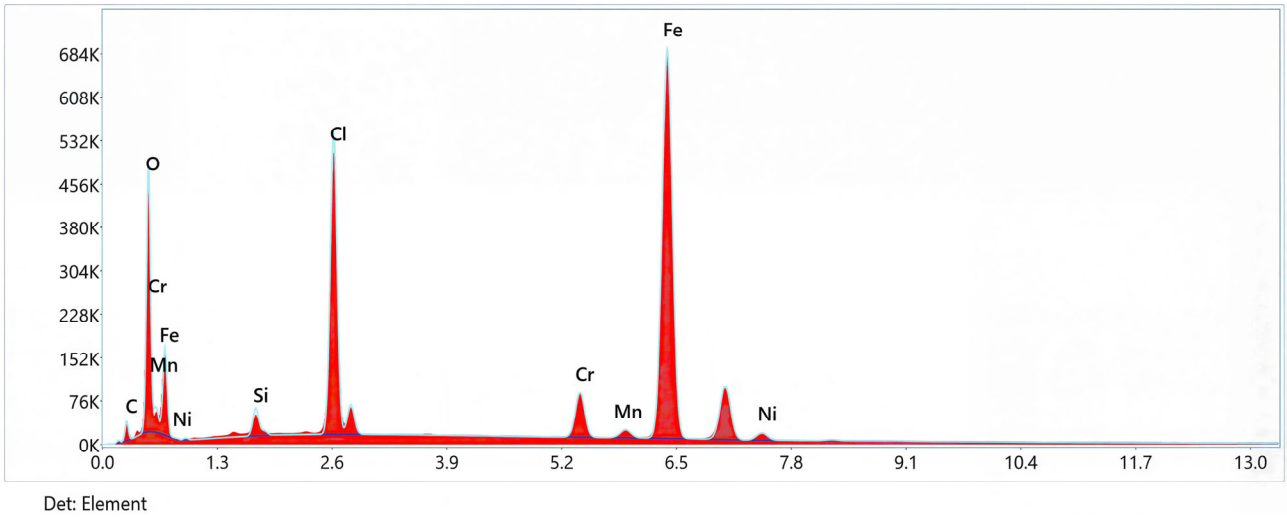

Fig. 12. Spectrum results from EDS, specimen preheat 180 °C.

B. *Mild Steel without Preheating and Stainless Steel with Preheat Treatment*

Tensile testing is conducted to assess the strength of the spot welding joint between mild steel and stainless steel materials. In this test, various treatments were applied to the material, namely without preheat treatment, as well as preheat at temperatures of 100 °C, 120 °C, 150 °C, and 180 °C. Each treatment involves testing on three specimens to obtain accurate and representative data. The tensile test data for the untreated mild steel plate and the AISI 304 stainless steel with preheating treatment are shown in Table III.

The tensile test results, detailed in Table III and Fig. 13, demonstrate that the strategic application of preheat exclusively to the stainless steel component significantly alters the mechanical properties of the dissimilar spot welds with mild steel. In the baseline condition, the joint exhibited high tensile strength (127.46 MPa) but low ductility, evidenced by a negative strain value of −0.69% GL. This mechanical behavior is characteristic of a rapid cooling cycle, which fosters the formation of hard, brittle microstructures such as martensite on the mild steel side. The negative strain is a critical indicator of significant tensile residual stress within the joint. This stress arises from the disparate thermal properties of the two materials, particularly the fact that austenitic stainless steel has a lower thermal conductivity and a higher coefficient of thermal expansion than mild steel. This differential causes the stainless steel to retain heat longer and contract more, leading to uneven cooling and imposing a state of residual tension on the joint, which manifests as apparent compressive strain during testing.

TABLE III. TENSILE TEST DATA FOR MILD STEEL WITHOUT PREHEATING AND STAINLESS STEEL WITH PREHEAT TREATMENT

Preheat	Variation Preheat	Specimen			Average	Standard Deviation
		1	2	3		
Without	Stress (MPa)	114.06	130.96	137.36	127.46	12.04
	Strain (%GL)	−0.88	−0.64	−0.56	−0.69	0.17
100 °C	Stress (MPa)	111.49	142.14	105.46	119.70	19.67
	Strain (%GL)	−0.88	−0.64	−0.56	−0.69	0.17
120 °C	Stress (MPa)	90.91	119.83	94.69	101.81	15.72
	Strain (%GL)	0.64	0.93	0.66	0.74	0.16
150 °C	Stress (MPa)	80.90	87.49	97.87	88.75	8.55
	Strain (%GL)	0.56	0.61	0.64	0.60	0.04
180 °C	Stress (MPa)	164.35	152.34	152.28	156.32	6.95
	Strain (%GL)	1.81	1.75	1.83	1.80	0.04

As the preheat temperature was elevated to intermediate levels (100 °C and 120 °C), a clear trade-off between strength and ductility was observed. The tensile strength decreased to 119.70 MPa and 101.81 MPa, respectively, while the strain became positive, increasing to 0.74% GL. This transition confirms that preheating effectively moderates the cooling rate, thereby reducing the thermal gradient and alleviating residual stresses, which in turn

permits greater plastic deformation. However, the persistently high standard deviations at these temperatures (19.67 MPa and 15.72 MPa) indicate an unstable thermal process. The heat input is sufficient to initiate microstructural changes but not enough to ensure consistent and homogeneous transformation across the weld zone, leading to high variability in mechanical performance.

The optimum condition was achieved at a preheat temperature of 180 °C. At this temperature, the joint attained the highest tensile strength (156.32 MPa), superior ductility (strain of 1.80% GL), and the lowest standard deviation (6.95 MPa). This combination of properties signifies a fundamental improvement in joint integrity. The 180 °C preheat is sufficiently high to effectively minimize the thermal gradient, substantially reduce residual stresses, and slow the cooling rate to prevent excessive martensite formation while promoting a more ductile microstructure. The low standard deviation underscores excellent process stability and microstructural homogeneity. Therefore, a preheat of 180 °C is identified as the optimal parameter, successfully balancing high strength with enhanced ductility and ensuring consistent, reliable weld performance.

The analysis of hardness distribution in the welded joint between untreated mild steel and preheated stainless steel was conducted to characterize the influence of varying preheat temperatures on the mechanical properties across three critical areas: the weld zone, HAZ, and base metal. Based on the data in Table IV, it was observed that the hardness values in each area responded differently to increasing preheat temperatures, reflecting microstructural changes occurring during the welding process.

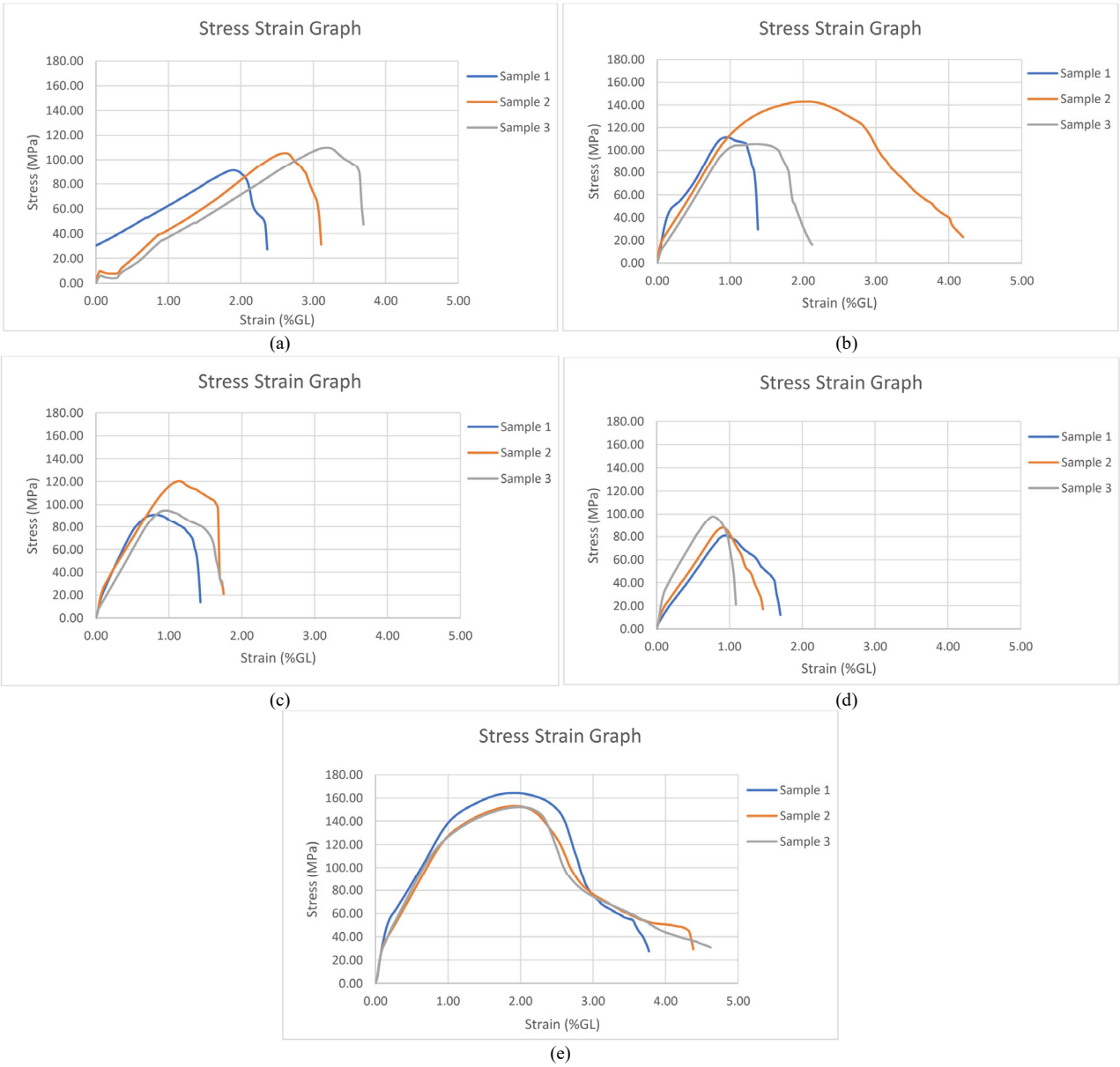

Fig. 13. Stress–strain graphs of welded specimens at different preheat temperatures. (a) Without preheat; (b) Preheat 100 °C; (c) Preheat 120 °C; (d) Preheat 150 °C; (e) Preheat 180 °C.

TABLE IV. HARDNESS TEST DATA OF MILD STEEL WELDING MATERIAL WITHOUT PREHEATING AND STAINLESS STEEL WITH PREHEAT TREATMENT

Preheat	Weld area (HRC)	Average	HAZ (HRC)	Average	Base Metal (HRC)	Average
Without	100.30	102.20	88.10	83.30	98.10	98.10
	102.10		86.50		96.10	
	104.20		75.30		100.10	
100 °C	109.20	108.20	79.40	88.80	90.60	86.70
	109.20		95.20		86.80	
	106.20		91.80		82.70	
120 °C	102.20	104.90	95.20	99.03	92.30	93.73
	102.20		99.80		90.00	
	110.30		102.10		98.90	
150 °C	94.20	100.83	86.60	89.93	71.10	80.03
	103.20		88.30		82.20	
	105.10		94.90		86.80	
180 °C	107.10	109.30	95.20	95.77	72.40	77.63
	114.90		98.20		73.70	
	105.90		93.90		86.80	

In the weld area, the average hardness values showed fluctuations with increasing preheat temperature. The highest hardness was achieved at 100 °C preheat (108.20 HRC) and 180 °C preheat (109.30 HRC), while the lowest value was observed at 150 °C preheat (100.83 HRC). This pattern indicates that preheating at 150 °C may have produced an optimal cooling rate to reduce the formation of hard and brittle martensitic phases, thereby decreasing hardness. However, the subsequent increase in hardness at 180 °C suggests that tempering processes or the formation of other secondary phases may have occurred. In the HAZ area, a clear trend of increasing average hardness was observed with rising preheat temperature, from 83.30 HRC (without preheat) to 95.77 HRC (at 180 °C). This increase may be caused by more complete tempering processes or phase transformations resulting in more stable and harder microstructures. Meanwhile, the stainless steel base metal showed a consistent trend of decreasing hardness with increasing preheat temperature, from 98.10 HRC to 77.63 HRC. This significant decrease is most likely caused by the annealing phenomenon, where heating to these temperatures softens the material by promoting recrystallization and reducing dislocations. Overall, this hardness data confirms that preheat treatment plays a crucial role in modifying the mechanical property gradient in dissimilar welded joints. The 180 °C preheat temperature shows the most balanced results with high weld hardness, hardened HAZ, and softer base metal, which ultimately may lead to improved overall joint performance.

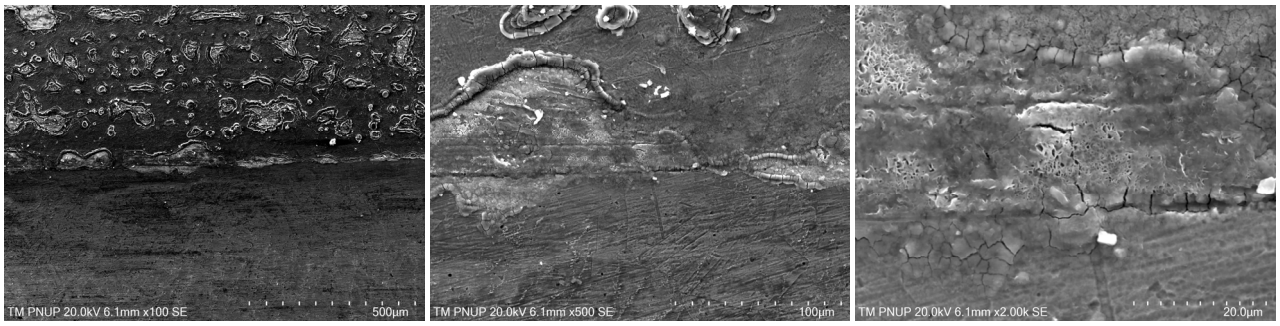

(a) (b) (c)

Fig. 14. SEM images of the specimen with 150 °C preheat at different magnifications. (a) 100× magnification; (b) 500× magnification; (c) 2000× magnification.

Fig. 14 presents a comprehensive SEM analysis of the spot weld joint between non-preheated mild steel and 150 °C preheated stainless steel, revealing significant microstructural evolution across multiple magnification scales. At 100× magnification, the fusion zone exhibits irregular boundaries and substantial surface heterogeneity, suggesting elemental segregation and phase transformation disparities at the material interface. These morphological characteristics indicate that despite the application of preheating, the solidification process remained non-uniform, resulting in microstructural inhomogeneity throughout the joint region.

Higher resolution imaging at 500× and 2000× magnification provides enhanced visualization of microcrack propagation along the interfacial region, particularly concentrated within areas exhibiting pronounced surface roughness and porosity. These discontinuities are attributed to the differential thermal expansion coefficients between the dissimilar materials, generating substantial residual stresses during the post-welding cooling phase. The concurrent presence of micropores and elemental segregation further compromises the interfacial bonding integrity between the two metals.

Advanced microstructural examination reveals the formation of brittle intermetallic compounds, predominantly resulting from complex Fe-Cr-Ni interactions within the fusion zone. While these phases

contribute to hardness enhancement, their inherent brittleness significantly diminishes the joint's mechanical performance and structural reliability. Collectively, these observations demonstrate that while the 150 °C preheat treatment provides partial mitigation of thermal stresses, it remains insufficient to prevent the formation of microcracks, elemental segregation, and brittle intermetallic phases, ultimately compromising the weld's structural integrity.

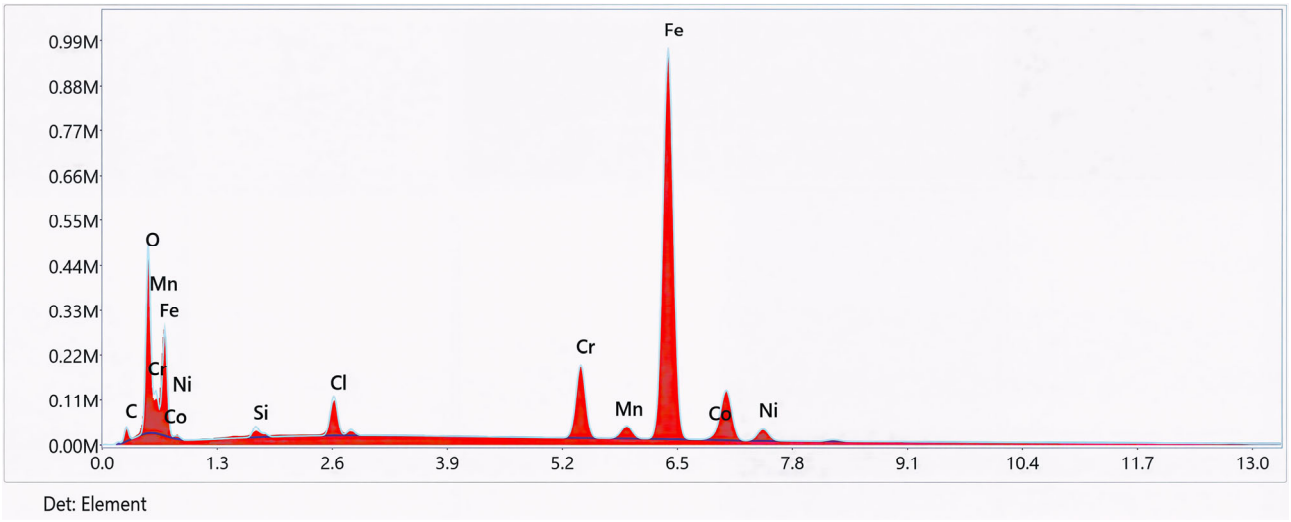

Fig. 15. Spectrum results from EDS, specimen preheat 150 °C.

EDS characterization of the dissimilar weld joint between mild steel and stainless steel shown in Fig. 15, processed with a 150 °C preheat treatment, reveals a complex elemental distribution within the fusion zone. Spectral analysis identifies Fe as the predominant constituent, evidenced by the characteristic peak at approximately 6.5 keV, consistent with its fundamental role in both base materials. The detection of C at 0.3 keV confirms its presence as a crucial strengthening element in the steel matrix.

The spectrum further verifies the successful integration of stainless steel alloying elements, with Cr identified at 5.4 keV and Ni detected at 7.5 keV, both essential for enhancing the joint's corrosion resistance and oxidative stability. Moderate Mn concentrations contribute to solid solution strengthening mechanisms, while trace elements including Cobalt (Co), Si, Cl, and O suggest potential exogenous contributions from processing environments or surface conditions.

The identification of oxygen signatures indicates limited oxidation during thermal cycling, while silicon and chlorine detection warrants further investigation into potential environmental interactions. This comprehensive elemental analysis demonstrates that preheating at 150 °C facilitates improved elemental distribution homogeneity across the fusion zone, ultimately contributing to enhanced mechanical integrity and corrosion performance in the resulting weldment.

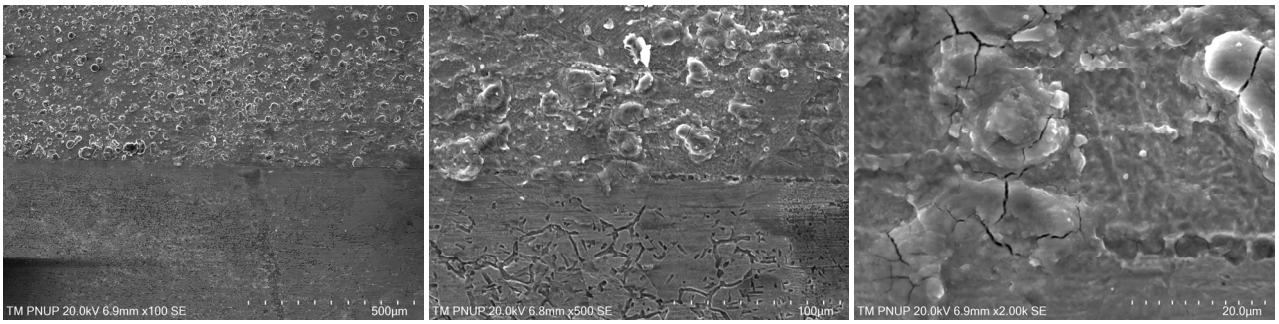

(a) (b) (c)

Fig. 16. SEM images of the specimen with 180 °C preheat at different magnifications. (a) 100× magnification; (b) 500× magnification; (c) 2000× magnification.

Fig. 16 presents the SEM analysis of a spot-welded joint between mild steel and stainless steel—the latter preheated to 180 °C—reveals that while preheating mitigated thermal gradients during welding, certain structural imperfections persisted. At 100× magnification, the joint exhibits a coarse microstructure with non-uniform oxide distribution and a distinct fusion boundary, suggesting constrained elemental diffusion and the potential for segregation or intermetallic compound formation in the transition zone. Under higher magnification (500×), microcracks adjacent to oxidized regions, along with minor porosity and inclusions, become more apparent; these features are likely detrimental to the joint's mechanical integrity. At this scale, the intermetallic phases

at the mild steel-stainless steel interface are also more clearly resolved.

Further examination at 2000× magnification highlights the predominance of microcracks and oxide particles, indicative of oxidation reactions and the formation of brittle intermetallic phases, potentially exacerbated by the mismatch in the materials' coefficients of thermal expansion. In conclusion, although preheating to 180 °C positively influences joint stability and reduces thermal stress, the presence of elemental segregation, porosity, and brittle phases continues to compromise the mechanical strength of the weld.

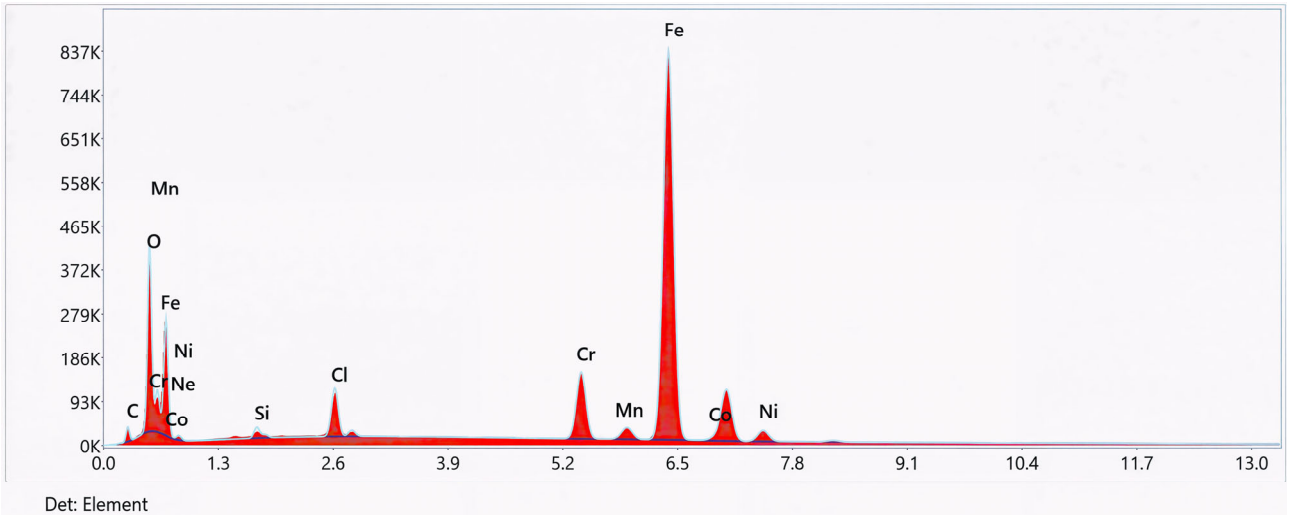

Fig. 17. Spectrum results from EDS, specimen preheat 180 °C.

The Scanning Electron Microscopy/Energy Dispersive Spectroscopy (SEM/EDS) spectra shown in Fig. 17 of the spot weld between mild steel (non-preheated) and stainless steel (preheated to 180 °C) delineate the distribution of principal elements within the joint. The spectrum is dominated by a prominent Fe peak, consistent with its prevalence in the mild steel base metal. Significant concentrations of Cr and Ni, constituents of the stainless steel, were also identified; these elements enhance corrosion resistance, mechanical strength, and high-temperature performance. The presence of Mn contributes to increased strength and wear resistance. A notable oxygen signal suggests some surface oxidation occurred during welding.

Critically, the C signal was weak, indicating minimal diffusion from the mild steel into the stainless steel. This limited carbon transport reduces the risk of chromium carbide precipitation, thereby mitigating the potential for sensitization and the consequent loss of corrosion resistance in the stainless steel. Trace amounts of Co and Cl were detected, likely as minor impurities.

The 180 °C preheat treatment appears to have promoted a more homogeneous elemental distribution. This homogenization mitigates residual stresses arising from the thermal expansion mismatch between the two materials, subsequently reducing crack susceptibility. Furthermore, the reduced cooling rate facilitated by preheating helps inhibit the formation of brittle microstructures, thereby enhancing the overall toughness of the weld joint. In summary, the 180 °C preheating contributes to microstructural stability, optimizes mechanical properties, and helps preserve the corrosion resistance of the welded joint.

IV. Conclusion

The implementation of a 150–180 °C preheating treatment for resistance spot welding of dissimilar joints between mild steel and stainless steel is strongly recommended for real-world applications in automotive and structural engineering. This approach shifts the focus from merely maximizing tensile strength to optimizing long-term joint integrity and reliability. The optimized preheating regime effectively reduces the cooling rate, thereby suppressing the formation of brittle martensite and alleviating residual stresses caused by the differences in thermal properties of the base metals. As a result, the weldment exhibits slightly lower ultimate strength but significantly enhanced ductility, microstructural homogeneity, and mechanical consistency. These improvements directly contribute to greater fatigue resistance under cyclic loading in automotive chassis and body structures, as well as enhanced resistance to stress-corrosion cracking and brittle fracture in critical structural components—ultimately ensuring improved in-service safety and durability.

The findings of this study further demonstrate that preheating stainless steel components prior to resistance spot welding with mild steel significantly improves joint quality by reducing residual stresses and enhancing ductility and microstructural uniformity. The optimal preheating temperature was determined to be 180 °C, achieving the best combination of high tensile strength (156.32 MPa), positive strain (1.80% GL), and low standard deviation, indicating both process stability and joint reliability. In practical applications, these results are particularly relevant to the automotive industry, which

frequently employs dissimilar metal joints in vehicle frames, body panels, and exhaust systems. By preheating stainless steel before welding, the risk of cracking due to differences in thermal conductivity can be minimized, leading to stronger, more durable joints and extended service life of the components.

CONFLICT OF INTEREST

The authors declare no conflict of interest.

AUTHOR CONTRIBUTIONS

KP conducted the research, performed the data analysis, and drafted the manuscript; NS, AYA, and AH supervised the research direction, guided the overall research process, and provided constructive feedback and revisions to improve the quality of the manuscript; all authors had approved the final version.

ACKNOWLEDGMENT

The authors would like to express their sincere gratitude to the Department of Mechanical Engineering, Hasanuddin University, and Universitas Kristen Paulus Makassar for their support and contributions to this research.

REFERENCES

[1] V. H. B. Hernandez, S. K. Panda, Y. Okita *et al.,* "A study on heat affected zone softening in resistance spot welded dual phase steel by nanoindentation," *J. Mater. Sci.,* vol. 45, no. 6, pp. 1638–1647, 2010. doi: 10.1007/s10853-009-4141-0

[2] I. Hajiannia, R. Ashiri, M. R. Pakmanesh *et al.,* "Evaluation of performance of resistance spot welded joints with different parameters in advanced high strength TRIP steel," *J. Environ. Friendly Mater.*, vol. 3, no. 1, pp. 9–16, 2019.

[3] M. S. M. Sani, N. A. Nazri, and D. A. J. Alawi, "Vibration analysis of resistance spot welding joint for dissimilar plate structure (mild steel 1010 and stainless steel 304)," in *IOP Conf. Ser. Mater. Sci. Eng.*, vol. 238, no. 1, 012017, 2017. doi: 10.1088/1757-899X/238/1/012017

[4] B. Wang, F. Qiu, L. Chen *et al.,* "Microstructure and shearing strength of stainless steel/low carbon steel joints produced by resistance spot welding," *J. Mater. Res. Technol.*, vol. 20, pp. 2668–2679, 2022. doi: 10.1016/j.jmrt.2022.08.041

[5] H. Moshayedi and I. Sattari-Far, "Resistance spot welding and the effects of welding time and current on residual stresses," *J. Mater. Process. Technol.*, vol. 214, no. 11, pp. 2545–2552, 2014. doi: 10.1016/j.jmatprotec.2014.05.008

[6] V. Onar and S. Aslanlar, "Welding time effect of welding joints in micro alloyed and TRIP 800 steels in resistance spot welding," *Acta Phys. Pol. A*, vol. 131, no. 3, pp. 389–391, 2017. doi: 10.12693/APhysPolA.131.389

[7] B. Wang, L. Hua, X. Wang *et al.,* "Effects of electrode tip morphology on resistance spot welding quality of DP590 dual-phase steel," *Int. J. Adv. Manuf. Technol.*, vol. 83, no. 9, pp. 1917–1926, 2016. doi: 10.1007/s00170-015-7703-0

[8] A. K. Biradar and B. M. Dabade, "Optimization of resistance spot welding process parameters in dissimilar joint of MS and ASS 304 sheets," *Mater. Today Proc.*, vol. 26, pp. 1284–1288, 2020. doi: 10.1016/j.matpr.2020.02.256

[9] T. Das, R. Das, and J. Paul, "Resistance spot welding of dissimilar AISI-1008 steel/Al-1100 alloy lap joints with a graphene interlayer," *J. Manuf. Process.*, vol. 53, pp. 260–274, 2020. doi: 10.1016/j.jmapro.2020.02.032

[10] D. Mishra, K. Rajanikanth, M. Shunmugasundaram *et al.,* "Dissimilar resistance spot welding of mild steel and stainless steel metal sheets for optimum weld nugget size," *Mater. Today Proc.*, vol. 46, pp. 919–924, 2021. doi: 10.1016/j.matpr.2021.01.067

[11] R. Qiu, J. Li, H. Shi *et al.,* "Characterization of resistance spot welded joints between aluminum alloy and mild steel with composite electrodes," *J. Mater. Res. Technol.*, vol. 24, pp. 1190–1202, 2023. doi: 10.1016/j.jmrt.2023.03.069

[12] W. Zhang, K. Zhang, Y. Yang *et al.,* "A novel dissimilar resistance spot welding of Ti6Al4V alloy and 316L stainless steel via copper as interlayer by using optimal electrodes," *J. Mater. Res. Technol.*, vol. 33, pp. 5425–5437, 2024. doi: 10.1016/j.jmrt.2024.10.183

[13] B. V. F. Kemda, N. Barka, M. Jahazi *et al.,* "Optimization of resistance spot welding process applied to A36 mild steel and hot dipped galvanized steel based on hardness and nugget geometry," *Int. J. Adv. Manuf. Technol.*, vol. 106, no. 5, pp. 2477–2491, 2020. doi: 10.1007/s00170-019-04707-w

[14] A. Arumugam and A. Pramanik, "A study of spot weld Pull-out Failure (PF) mechanism under different loading conditions for stainless steel and mild steel joints," *Aust. J. Mech. Eng.*, vol. 20, no. 3, pp. 603–616, 2022. doi: 10.1080/14484846.2020.1725348

[15] M. S. Sukardin, I. Renreng, H. Arsyad *et al.,* "Optimization of resistance spot welding with surface roughness dissimilar mild steel with stainless steel," *Eastern-European J. Enterp. Technol.*, vol. 125, no. 12, pp. 63–71, 2023. doi: 10.15587/1729-4061.2023.285711

[16] C. Zhu, X. Tang, Y. He *et al.,* "Effect of preheating on the defects and microstructure in NG-GMA welding of 5083 Al-alloy," *J. Mater. Process. Technol.*, vol. 251, pp. 214–224, 2018. doi: 10.1016/j.jmatprotec.2017.08.037

[17] S. Raj and P. Biswas, "Effect of induction preheating on microstructure and mechanical properties of friction stir welded dissimilar material joints of Inconel 718 and SS316L," *CIRP J. Manuf. Sci. Technol.*, vol. 41, pp. 160–179, 2023. doi: 10.1016/j.cirpj.2022.12.014

[18] S. Raj and P. Biswas, "High-frequency induction assisted hybrid friction stir welding of Inconel 718 plates," *J. Manuf. Sci. Eng.*, vol. 144, no. 4, 2022. doi: 10.1115/1.4052357

[19] C. Köse and R. Kaçar, "The effect of preheat & post weld heat treatment on the laser weldability of AISI 420 martensitic stainless steel," *Mater. Des.*, vol. 64, pp. 221–226, 2014. doi: 10.1016/j.matdes.2014.07.044

[20] Z. Luo, S. Ao, Y. J. Chao *et al.,* "Application of pre-heating to improve the consistency and quality in AA5052 resistance spot welding," *J. Mater. Eng. Perform.*, vol. 24, no. 10, pp. 3881–3891, 2015. doi: 10.1007/s11665-015-1704-x

[21] M. R. Mohamad, L. H. Shah, and M. Ishak, "Investigation of preheating method on joint strength of aluminium-stainless steel dissimilar welding using Metal Inert Gas (MIG) process," *in IOP Conf. Ser. Mater. Sci. Eng.*, vol. 238, no. 1, 2017. doi: 10.1088/1757-899X/238/1/012019

[22] S. Kumar and R. Singh, "Investigation of tensile properties of shielded metal arc weldments of AISI 1018 mild steel with preheating process," *Mater. Today Proc.*, vol. 26, pp. 209–222, 2019. doi: 10.1016/j.matpr.2019.10.167

[23] M. Jawad, M. Jahanzaib, M. A. Ali *et al.,* "Revealing the microstructure and mechanical attributes of pre-heated conditions for gas tungsten arc welded AISI 1045 steel joints," *Int. J. Press. Vessel. Pip.*, vol. 192, 104440, 2021. doi: 10.1016/j.ijpvp.2021.104440

[24] D. Wicaksono, M. N. Ilman, and N. A. Triwibowo, "Effect of preheating on mechanical properties and corrosion behavior of dissimilar GMAW joints between austenitic stainless steel and low carbon steel," in *Proc. American Institute of Physics Conf. Series*, 2023, vol. 2592, no. 1, 30013.

[25] S. Kumar and R. Singh, "Optimization of process parameters of metal inert gas welding with preheating on AISI 1018 mild steel using grey based Taguchi method," *Meas. J. Int. Meas. Confed.*, vol. 148, 106924, 2019. doi: 10.1016/j.measurement.2019.106924

[26] M. Mazni, M. H. B. Ismail, H. F. B. Pahroraji *et al.,* "Effect of welding preheats on metallurgical analysis and microstructural development," in *IOP Conf. Ser. Mater. Sci. Eng.*, vol. 834, no. 1, 012045, 2020. doi: 10.1088/1757-899X/834/1/012045

[27] Sudarsono, A. Arifin, Gunawan *et al.,* "The effect of preheating on the mechanical properties of AISI 1037 and AISI 304 welded joints using shielded metal arc welding," *Materials (Basel).*, vol. 17, no. 23, 2024. doi: 10.3390/ma17235780

[28] Z. Dou, S. Li, Y. Zhao *et al.,* "Microstructure and mechanical properties of a preheating friction stir welded beryllium aluminum casting alloy," *Welding in the World*, pp. 11–4, 2025. doi: 10.1007/s40194-025-02179-z

[29] J. He, M. Wei, L. Zhang *et al.,* "Effect of preheat temperature and welding sequence on the temperature distribution and residual stress in the weld overlay repair of hydroturbine runner," M*aterials (Basel)*., vol. 15, no. 14, 4867, 2022. doi: 10.3390/ma15144867

[30] M. A. M. Shah, F. H. Rosli, B. Abdullah *et al.,* "Effect of different preheating's temperature towards the integrity of weldment AISI 1045," in *IOP Conf. Ser. Mater. Sci. Eng.*, vol. 834, no. 1, 012070, 2020. doi: 10.1088/1757-899X/834/1/012070

[31] S. H. M. Anijdan, M. Sabzi, M. Ghobeiti-Hasab *et al.,* "Optimization of spot welding process parameters in dissimilar joint of dual phase steel DP600 and AISI 304 stainless steel to achieve the highest level of shear-tensile strength," *Mater. Sci. Eng. A*, vol. 726, pp. 120–125, 2018. doi: 10.1016/j.msea.2018.04.072

[32] D. A. College, "Analysis of spherical indenter rockwell superficial hardness tests on thin annealed low-carbon steel," *J. Mater. Eng. Perform.*, vol. 32, no. 7, pp. 2892–2905, 2023. doi: 10.1007/s11665-022-07303-4

[33] S. S. R. Singh, R. V. Praneeth, V. S. Sankalp *et al.,* "Welding, mechanical properties and microstructure of different grades of austenitic stainless steels: A review," *Mater. Today Proc.*, vol. 62, pp. 3675–3680, 2022. doi: 10.1016/j.matpr.2022.04.425

[34] V. Feizollahi, A. Bahmani, N. Nadimi *et al.,* "Factors affecting weld quality in resistance spot welding of advanced high strength steels," *Sci. Rep.*, vol. 15, no. 1, 30012, 2025. doi: 10.1038/s41598-025-14174-x

[35] M. Alali and M. G. Alnaffakh, "Characterization of AISI 316L stainless steel/low alloy steel resistance spot dissimilar weld," *Metallogr. Microstruct. Anal.*, vol. 12, no. 4, pp. 622–633, 2023. doi: 10.1007/s13632-023-00990-y